



This article appeared in a journal published by Elsevier. The attached copy is furnished to the author for internal non-commercial research and education use, including for instruction at the authors institution and sharing with colleagues.

Other uses, including reproduction and distribution, or selling or licensing copies, or posting to personal, institutional or third party websites are prohibited.

In most cases authors are permitted to post their version of the article (e.g. in Word or Tex form) to their personal website or institutional repository. Authors requiring further information regarding Elsevier's archiving and manuscript policies are encouraged to visit:

<http://www.elsevier.com/copyright>



Contents lists available at ScienceDirect

Chemical Physics

journal homepage: www.elsevier.com/locate/chemphys

A model for the multi-exponential excited-state decay of CdSe nanocrystals

A. Al Salman^a, A. Tortschanoff^a, G. van der Zwan^b, F. van Mourik^a, M. Chergui^{a,*}^aLaboratoire de Spectroscopie Ultrarapide, Ecole Polytechnique Fédérale de Lausanne, ISIC-FSB-BSP, CH-1015 Lausanne, Switzerland^bLaser Centre VU, Analytical Chemistry and Applied Spectroscopy, Faculty of Sciences, Vrije Universiteit Amsterdam, de Boelelaan 1083, 1081 HV Amsterdam, The Netherlands

ARTICLE INFO

Article history:

Received 4 July 2008

Accepted 17 October 2008

Available online 5 November 2008

Keywords:

Cadmium selenide

Nanoparticles

Electron–hole recombination

Nanosecond kinetics

Dipole moments

ABSTRACT

We report on photoluminescence decay measurements of CdSe nanoparticles over several decades of intensities and times, and as a function of size and temperature. A model is proposed for the multi-exponential decay kinetics, and their temperature dependence, in which a major role is played by the now well established presence of a large ground-state dipole moment in CdSe nano crystals. By two-photon excitation within the bandgap region we show that there is a link between the ground-state dipole moment and the excited-state decay. The stochastic nature of the magnitude of the dipole moment results in a complex temperature dependence. Contrary to studies that ascribe non-radiative decay processes to surface states/traps, the mechanism we propose considers the intrinsic states described within the effective mass approximation models for the spectroscopy of the bandgap. Surface effects are mediated by the ground-state dipole moments that they constitute, which in turn perturb the intrinsic states.

© 2008 Elsevier B.V. All rights reserved.

1. Introduction

The spectroscopy of semiconductor nanocrystals is of considerable interest in view of many potential applications. The most common theoretical description of the electronic structure of the bandgap of CdSe nanocrystals uses the effective mass approximation [1]. In this model the basic excitonic structure is simply described as the product of Bloch functions and an envelope function which confines the electron and hole to a spherical well. However, due to the requirement of using eigenfunctions of the total angular momentum operator, together with a variety of symmetry breaking effects, it still leads to a relatively complex set of states and transitions for the bandgap region. The model correctly describes most spectroscopic properties of the particles. A good example is the temperature dependence of the luminescence at temperatures below 10 K, caused by the equilibrium between dark and bright excitons [2,3]. Phenomena that are not well described by the model are the multi-exponential decay kinetics of the excited state(s) [4], and the observation of large ground-state dipole moments in these particles [5–7]. From a spectroscopic point of view the dipole moment is thought to be responsible for breaking the inversion symmetry of the lattice, making the bandgap transitions partly two-photon allowed [6]. From our electric linear dichroism (LD) experiments we concluded that there are also significant changes in the dipole strength and energies of some of the bandgap transitions [7].

Fig. 1 gives a schematic overview of the level scheme of the bandgap transitions, and of the modifications that are induced by the ground-state dipole moment, based on our LD experiments and calculations [7]. The states are labelled according to F , the total angular momentum projected on the crystallographic axis (z -axis). There are two transitions to/from states with zero angular momentum along the z -axis, labelled $F=0^U$ and $F=0^L$ (U, L : upper and lower), of which the 0^L has no dipole strength.

The lowest state is twofold degenerate, and is optically forbidden since it corresponds to a change in angular momentum along the z -axis of ± 2 . The $\pm 1^U$ and $\pm 1^L$ are also twofold degenerate, and are both optically allowed. For small particles the $F=\pm 1^U$ is the dominant transition, while the $F=\pm 1^L$ transitions gain in relative intensity for larger particles. As can be seen, only the 0^U and 0^L transitions are polarized along the z -axis, and only these transitions are affected by the field of a dipole moment oriented along this axis by means of the coupling between the transition dipole moment and the ground-state dipole. For the larger particles, (diameter >4 nm) where the field of the dipole moment is relatively weak, we could quantitatively describe the effects, by only taking into account the mixing of p-hole and p-electron states into the 0^U and 0^L states (where s and p refer to the envelope function of the wavefunctions) [7]. This way the 0^{UL} transitions gain dipole strength by intensity borrowing from intraband transitions. For large particles the $F=0$ transitions gain about 10% in dipole strength, and red-shift. For the smaller crystals the changes in the dipole strength of the 0 transitions that we deduced from the LD spectra were too large to be covered by this approach, but the trends indicated in Fig. 1 were observed for all particle sizes.

* Corresponding author. Tel.: +41 21 693 0457/0447; fax: +41 21 693 0422.

E-mail address: Majed.Chergui@epfl.ch (M. Chergui).

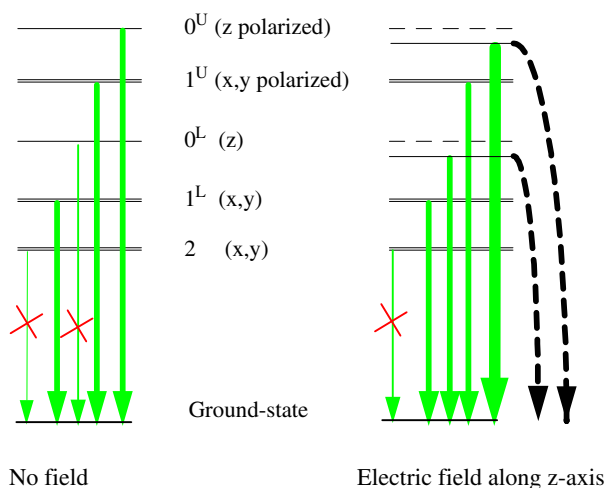


Fig. 1. Left: schematic representation of the fine splitting of the bandgap transitions of CdSe nanocrystals, as given by the “Efros” model [2] (The splittings between the levels are not scaled to relate to a specific particle size). Right: schematic representation of the influence of a strong electric field along the z -axis (the crystallographic axis) on the positions and strengths of the optical transitions (shown as emission) [7]. The dashed arrows represent non-radiative decay channels induced by the electric field, as discussed in the text.

In this work we propose that the 0^U and 0^L states could be responsible for non-radiative recombination processes, as indicated in Fig. 1. The stochastic nature of the magnitude of the ground-state dipole moments results in non-exponential fluorescence decay kinetics.

Two explanations have been proposed for the origin of the dipole moment; it could be due to a deviation from the ideal wurtzite crystal structure [8,9], or it could be due to imperfect termination of the crystals [9]. The first explanation predicts a dipole moment that scales with the volume of the particle, whereas the second explanation predicts a stochastic distribution. This explanation seems to work well for nanorods, where the volume is obviously much larger compared to spherical ones [8]. In our LD experiments [7] we found the largest dipole moments for the smaller nanocrystals, a strong indication that the dominant contribution for the dipole moment comes from imperfect termination of the crystals. Other support for this notion comes from the observation of ground-state dipole moments in ZnSe nanocrystals which have a zinc-blende structure, and can only obtain a dipole moment by this mechanism [6]. Here we make a link between the observed effects of the ground-state dipole moment on the spectroscopy of CdSe nanoparticles, and the nanosecond recombination kinetics.

2. Materials and methods

Spherical CdSe colloidal nanocrystals (size range of 2–4 nm diameter), were prepared by the method of Talpin et al. [10]. This method provides highly mono-disperse and fluorescent nano crystals (size distribution $\sim 5\%$, and fluorescence quantum yield $\sim 35\%$). The samples of different size were obtained from the same synthesis at regular time intervals during growth. The dots were dissolved in toluene, and their size was estimated from the position of the first exciton peak according to the calibration tables given by Peng et al. [11], and cross-checked by transmission electron microscopy (TEM). For comparison, the experiments were also performed on commercially available samples (evident technologies), giving identical results. For the measurements, the optical density at the excitation wavelength (400 nm) was adjusted to be identical for all the samples, ensuring a similar number of the absorbed photons. The samples were excited by the frequency-doubled output

of an amplified Ti-Sapphire laser (Coherent Rega 9050, repetition rate 250 kHz). The fluorescence was collected at 90° and the fluorescence of the sample was imaged onto a monochromator (CVI-Digikrom-CM110) with a bandwidth of 1 nm, and detected using a Microchannel plate photomultiplier (Hamamatsu Ru551). We used a GG420 filter to suppress the scattered 400 nm light. The solution was circulated inside a 0.5 mm thick quartz flow cell at a speed of 1 m/s to ensure constant renewal of the sample. For low temperature measurements, the samples were dried on a CaF_2 window attached to the cold finger of a liquid helium cooled cryostat (Oxford Instruments microstat). The focal spot size was determined to be $60 \mu\text{m}$ using a beam profiler. A time correlated single photon counting (TCSPC) apparatus with 65 ps instrument time resolution [full width at half maximum (FWHM)] was used to measure the decay kinetics. The one-photon measurements were all carried out at laser pump powers well below 0.05 W/cm^2 , ensuring that less than one exciton per particle is formed. For excitation in the bandgap area we used two optical parametric amplifiers pumped by the amplified Ti-Sapphire laser, a Coherent OPA9450 for the visible excitation, and a Coherent OPA9850 for the two-photon excitation.

3. Results and discussion

Fig. 2 shows a set of kinetic traces of 3.7 nm diameter CdSe nanocrystals at different temperatures. The traces were best fitted with four lifetimes. The four lifetimes are required to get a reasonable fit, fits using stretched exponentials were not as good. The lifetimes and amplitudes are represented in Fig. 3. The trends in the data are not too different from previously published results [12–14]. Note however, that contrary to the latter we systematically perform the measurements over a dynamic range of four orders of magnitude. The temperature dependence is rather complex. The shortest lifetime ($1.5 \pm 0.3 \text{ ns}$) did not show a clear temperature dependence. At very low temperatures the lifetimes increase, which has been well described by the dark exciton model, wherein the excitons get trapped in the optically forbidden $F = \pm 2$ states [2]. The lowest temperature reached in our experiments, 4.2 K, does not allow us to observe the longest radiative lifetimes reported for the $F = \pm 2$ states [2]. At intermediate temperatures there is the phenomenon of anti-quenching [15,6], especially affecting the longest component. It increases slightly with temperature around 100–150 K, and then decreases again at higher temperatures.

At this point, we do not attempt a description of all the contents of Fig. 3, which mostly serves as a reminder of the complexity of

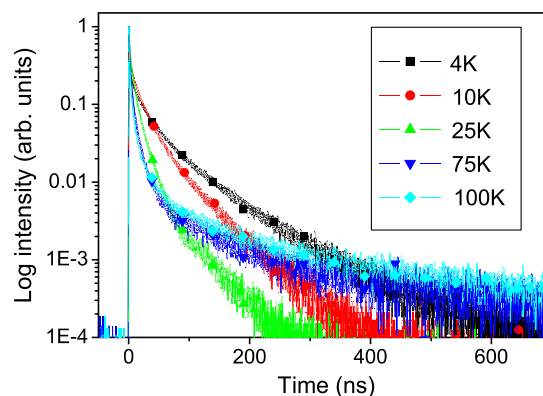


Fig. 2. Fluorescence decay curves of 4 nm diameter CdSe quantum dots, at different temperatures, excited at 400 nm. Detection was performed at the fluorescence maximum, which varies with temperature [4,12].

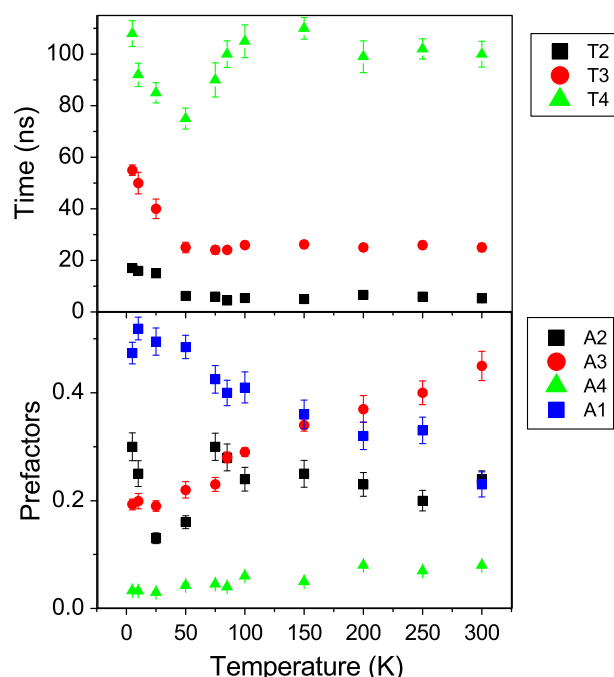


Fig. 3. Decay times (upper panel) and exponential prefactors (lower panel) as a function of temperature, obtained from a 4-exponential fit of the temperature dependent fluorescence decays (curves of Fig. 2a). The shortest lifetime was fixed at 1.5 ns.

the temperature dependence. A systematic study of the temperature dependence of many sizes and different nanoparticle preparation procedures always gave similar results with kinetics requiring at least four decay constants for a good fit [4].

At low temperatures (and probably also at room temperature under low fluence conditions that cannot be attained in single particle experiments) multi-exponential decays can only reflect heterogeneity of the sample. It has been shown that the heterogeneity and especially the overall quantum yield of luminescence is linked to surface effects [16]. Consequently non-radiative quenching is often explained by surface states [17], due to imperfections of the surface, which act as traps. Especially the anti-quenching effect [15,18] is interesting, it was shown that part of the temperature dependence of the non-radiative decay followed the phase transitions of the capping material [15]. This indicates that the surface states acting here are not due to chemical contaminations, but more likely involve rearrangements of the surface structure.

The surface is also thought to be the dominant cause for the large ground-state dipole moments observed for these particles [7,19]. Indeed, from our LD experiments we concluded that the dipole moments did not scale with the volume of the particles, and were too large to be due to a lattice effect [7]. Therefore the dipole moments must be due to the imperfect termination of the particles [8].

As we have demonstrated, the dipole moments introduce a characteristic perturbation to the spectroscopy of the particles, more specifically, the optical transitions that are polarized along the direction of the dipole moment, 0^U and 0^L , are strongly perturbed.

Guyot-Sionnest and co-workers [6] interpreted the fact that their two-photon and one-photon excitation profiles of the band-gap region are identical, as evidence that the field of the dipole moment makes the bandgap transitions (weakly) two-photon allowed. Our LD experiments are more specific, since they indicate that the ground-state dipole moments are oriented along the crystallographic axis of the particle and consequentially, only the 0^U

and 0^L transitions couple with this field. However, we also found that the transitions polarized along the z-axis were strongly red-shifted from their positions predicted by the Efros model. This explains why the two-photon excitation experiment [6] did not indicate the identity of the transition, because there is no splitting between the 0 and the ± 1 transitions.

Therefore, we think that the link between the spectroscopy and “surface states” is through the field of the ground-state dipole moment. It is natural to propose at this point that the dipole moment also plays a role in the non-radiative recombination processes. This connection is established next by comparing the photoluminescence decay kinetics for one- and two-photon excitation.

Fig. 4 shows the decay curves obtained upon excitation in the bandgap transition, and at higher energies. Clearly there are no significant differences between the two cases. Therefore, excitation with a large amount of excess energy does not affect the kinetics on a nanosecond time-scale, and all equilibration dynamics between the electronic levels within the nanocrystals are outside the temporal window of the experiments described here [20].

In Fig. 5 we compare 400 and 800 nm (two-photon) excitation, both at low and room temperature. Again, no clear differences are visible. However, note that at both temperatures the curves corresponding with 800 nm (two-photon) excitation are below the curves obtained with 400 nm excitation, indicating that the rela-

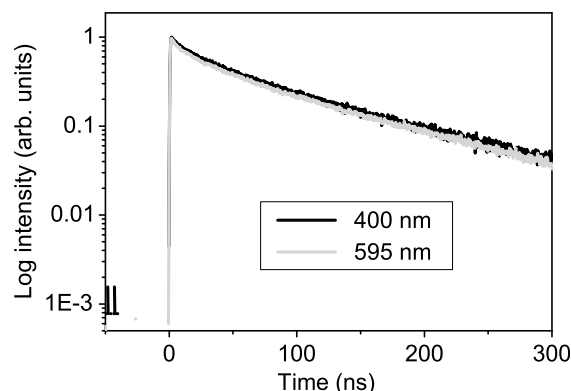


Fig. 4. Comparison of the room temperature fluorescence decay of a 4 nm CdSe QD for two different excitation energies: far above the bandgap (400 nm, black line), and resonant with the bandgap (595 nm, grey line). Detection was performed at the fluorescence maximum (617 nm).

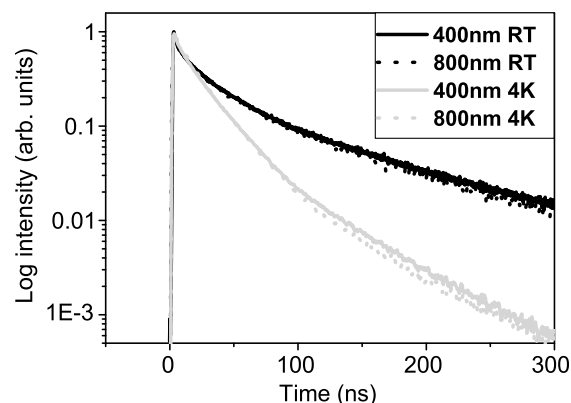


Fig. 5. Comparison of fluorescence decay kinetics of a 3.7 nm CdSe QD after excitation far above the band-edge with 100 fs 400 nm pulses (straight lines), and via two-photon excitation with 100 fs 800 nm pulses (dotted lines) at 4 K (grey curves), and at room temperature (black curves). Detection was at the fluorescence maximum (570 nm at 4 K and 585 nm at room temperature).

tive amplitude of the faster decay components is slightly higher for two-photon excitation.

Fig. 6 compares one and two-photon excitation, at the bandgap-transition energy. This time there is a significant difference between the two traces. In the case of two-photon excitation the relative amplitudes of the fast decay components are higher than in the case of one-photon excitation. All decay times are slightly shorter for two-photon excitation, indicative of enhanced non-radiative decay in the case of two-photon excitation. Note that we do not assign any specific meaning to the lifetimes obtained with the 3-exponential fit, they are used to describe non-exponential decays. A fit with 3 exponentials was used here because the dynamic range, and the time-window of the 2-photon excitation experiments were limited as compared to those of the data in Fig. 2 (where we needed 4 exponentials for a good fit).

Fig. 7 shows a zoom of the decay kinetics measured with higher time resolution. It is clear that with resonant two-photon excitation there is a decay component on a sub-ns time scale, which is barely seen under one-photon excitation. Note that there are no rise times in the emission after two-photon absorption, i.e. there is no long lived ($> \sim 20$ ps) dark state that is excited with two photons. This is in agreement with the two-photon excitation work of Schmidt et al. [6], who conclude that bandgap excitation with two

photons excites the bright (one-photon allowed) bandgap states, which have acquired some two-photon cross-section due to the polar lattice/ground-state dipole.

Why is there a difference between the two-photon and one-photon excitation curves in Figs. 6 and 7, whereas in Figs. 4 and 5 they are indistinguishable? The difference between the experimental conditions is that in the case of two-photon excitation outside the bandgap region there is an abundance of states that can be excited with one or two photons, i.e. the excitation process is not selective. Contrary to this, in the bandgap region two-photon excitation is only allowed as a result of the perturbation of the transitions/states caused by the ground-state dipole moment [6]. If we now consider the proposed mechanism for the formation of this ground-state dipole moment, imperfect termination of the crystal, it is natural to presume that the magnitude of the dipole moment is heterogeneous/stochastic. The single particle Stark experiments in Ref. [21], wherein the field sensitivity varies strongly between particles, are a clear manifestation of this heterogeneity. Therefore, two-photon excitation in the bandgap region selects those crystals from the ensemble that have a large dipole moment. The link between the ground-state dipole moment and the spectroscopy of the particles was already well established [5,7], but these observations finally make the link between the dipole moments and the kinetics.

In the literature, the non-radiative recombination processes are generally described by trapping to surface states, i.e. states not related to the electronic states/levels derived from the Efros model. We have shown here that there is a link between the two-photon cross-section of a particle and the presence of non-radiative recombination processes. The two-photon cross-section is not directly related to surface states, it is the result of a polar lattice, or a ground-state dipole moment which breaks the inversion symmetry of the lattice [6]. Since the measured ground-state dipole moments we found to be much larger than the lattice contribution [7], the former represents the major contribution. Therefore, two-photon excitation is selective for particles with a large ground-state dipole. Since the dipole moment is due to surface effects, we have not eliminated the possible role of “surface states” in the non-radiative recombination processes. However, we prefer a discussion of the effects in terms of the intrinsic optical transitions and dipolar properties of the particles. In our previous work we have shown how we can qualitatively model the effect of the ground-state dipole on the optical transitions. As a result, we found that 0^U and 0^L states become mixed states. In the Efros model, the bandgap states are all composed of s-type envelope functions, both for the hole and the electron states. When the electric field of the ground-state is taken into account, nearby p-electron and p-hole states get mixed into the 0^U and 0^L states [7]. As a result the 0^U and 0^L transitions gain dipole strength, which can be seen as intensity borrowing from the corresponding intraband transitions between the s- and p-states, and the transitions are red-shifted. Without proposing a specific model or mechanism at this point we just want to point out that the mixed nature of these modified 0^U and 0^L states should open up a wide range of possible (Auger) relaxation pathways.

In this picture the complexity of the decay kinetics and its temperature dependence is no longer a big surprise. The ground-state dipole moment is a stochastic property, the variability of the dipole moment should first of all give rise to a distribution in the splitting of the energy levels. For all particles where the energy levels of the $F = 0$ transitions are above the $\pm 1^L$ and ± 2 levels the quenching will be temperature activated, i.e. it can be frozen out. Moreover, the activation energy will be a distribution, leading to a complex temperature dependence, and multi-exponential decays at all temperatures. The sub-nanosecond decay component observed in Fig. 7 could be due to that fraction of the particles in which the activation barrier is absent because the quenching state is shifted below the other bandgap levels.

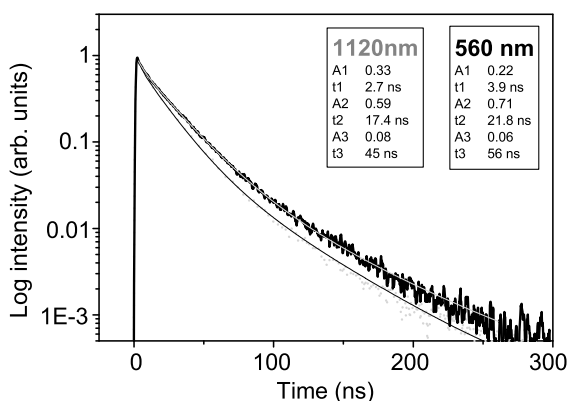


Fig. 6. Fluorescence decay kinetics of a CdSe QD at 4 K after resonant excitation into the bandgap with one-photon (560 nm, black line) or two-photon excitation (1120 nm, grey line). Insets show the decay times and amplitudes obtained from a 3-exponential fit. Fluorescence was detected at 575 nm.

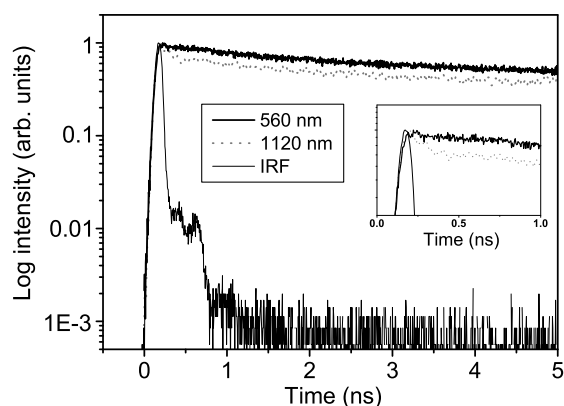


Fig. 7. Initial fluorescence decay kinetics measured in a reduced temporal window after resonant excitation into the bandgap: excitation with 560 nm (black line) and two-photon excitation with 1120 nm (grey line). The thin line indicates the instrument response function (IRF). The inset shows the short time behavior. Fluorescence was detected at the maximum of the emission spectrum (575 nm) for two-photon excitation and slightly on the red side (585 nm) in the case of one-photon excitation to avoid scattered excitation light.

At this point it is good to discuss some of the phenomena that are generally ascribed to surface states.

Many studies have appeared which relate the blinking of nanocrystals in single crystal photoluminescence studies to the multi-exponential recombination kinetics [22–24]. We would like to stress that the effects discussed here are not necessarily related to the charging effects observed in these single particle photoluminescence experiments. The single particle experiments described in [22] showed that single particles could switch between different states with different kinetics and fluorescence quantum yields, possibly due to charging effects. Although obviously related to the issues at hand here, there is a difference: Single particle experiments suffer from over-excitation of the studied object, and the blinking behavior that is observed does not necessarily relate to the multi-exponential decays observed in measurements on ensembles of particles. Our experiments were performed at a light flux that is at least four orders of magnitude lower than that used in single particle experiments. According to the dielectric dispersion experiments of Ref. [5], CdSe nanocrystals do not have a significant net charge in solution under normal illumination conditions.

From their measurements of the size and surface treatment dependence of the excited-state absorption in the gain region, Klimov and co-workers [25] concluded that these effects are not intrinsic to the nanocrystals. Their conclusion is mostly based on the size dependence of the excited-state absorption that occurs in the gain region (i.e. that prohibits the use of these particles as a laser gain medium). The excited-state absorption was especially prominent in the smaller particles, suggesting that the ratio between surface and volume could play a role. We observed a similar size dependence for the magnitude of the ground-state dipole moment in our LD experiments. However, in our experiments the large dipole moments are correlated with a large increase in the intrinsic absorption polarized parallel to the crystal axis. We consider it more likely that the excited-state absorption observed in Ref. [25] is related to a perturbation (by the ground- or excited-state dipole moment) of an intrinsic state of the particles.

In their single particle Stark fluorescence study Park et al. [21] also make the link between non-radiative decay and electric fields. However, they ascribe the effect to reversible trapping by charge-transfer states, i.e. to surface states/traps. The model they present has some similarities with Fig. 1, it requires a trap state situated at a slightly higher energy than the lowest intrinsic states of the particle. The field sensitivity of the trap state comes from its charge transfer nature, i.e. the energy level of the state is modified by the external field. As we have shown in our previous paper [7], the $F=0$ states are shifted to lower energies by an electric field (the dipole field), i.e. no extrinsic state is required, the scheme described in Fig. 1 is sufficient to explain these results.

Our intrinsic versus extrinsic arguments are not just semantics. Indeed, without surface effects there would not be a significant ground-state dipole moment, so one can ascribe everything to surface “states”. However, it appears that the perturbations caused by the surface effects are very specific: they are limited to the $F=0$ transitions, while other states are not affected. How could the dark exciton maintain its microsecond radiative lifetime in the presence of a perturbation that changes the dipole strength of a nearby transition by 10–100%? This is only possible if the perturbation is indeed by a field that is parallel to the crystallographic axis of the wurtzite crystal. Therefore we consider the quenching state as an intrinsic property of the particle.

This raises another issue, since there are also semiconductor nanocrystals that do not have the wurtzite structure. Also in these particles large ground-state dipole moments have been found [5,9,26], and multi-exponential decays have been reported [27]. We performed a comparative study of wurtzite and zincblende

CdSe nanocrystals, and found no significant differences either in the high-resolution spectroscopy or in the temperature dependence of the decay kinetics [28]. Given the central role of the crystal field splitting in the Efros model for the wurtzite crystals, it is surprising that this can happen. On the other hand, since also zincblende crystals generally have a ground-state dipole moment [19,26], this dipole moment could take over the role of the crystal field splitting in determining the fine structure of the bandgap [28].

4. Conclusions

We have found a correlation between the two-photon excitation cross-section of the bandgap transitions in CdSe nanocrystals and the non-radiative decay channels responsible for the multi-exponential decay kinetics. This correlation can be understood within the framework of our previous LD experiments [7], which showed a strong perturbation of the $F=0$ transitions due to the field of the ground-state dipole moment of the nanocrystals. We previously proposed a mechanism for the observed changes in the dipole strength of the $F=0$ transitions [7]. This mechanism involved the mixing of p-electron and p-hole wavefunctions into the s-electron and s-hole wave-functions of the $F=0$ transitions. Here we propose that the mixed nature of the $F=0$ states also underlies the (highly variable) non-radiative recombination processes in these particles. The ground-state dipole moment also causes a lowering of the energy of the $F=0$ states [7], which results in a lowering of the activation energy of the non-radiative recombination processes. Due to the stochastic nature of the magnitude of the ground-state dipole [19,21], this causes a complex temperature dependence of the photoluminescence kinetics. Although our model implicitly depends on the surface effects that cause the ground-state dipole moment, no surface states are involved in the spectroscopy or the dynamics.

Acknowledgements

This work was supported by the Swiss National Science Foundation (Project No. 200020-105333) and by the NCCR Quantum Photonics program.

References

- [1] A.L. Rosen, M. Efros, *Ann. Rev. Mater. Sci.* 30 (2000) 475.
- [2] A.L. Efros, M. Rosen, M. Kuno, M. Nirmal, D.J. Norris, M. Bawendi, *Phys. Rev. B* 54 (1996) 4843.
- [3] M. Nirmal, D.J. Norris, M. Kuno, M.G. Bawendi, A.L. Efros, M. Rosen, *Phys. Rev. Lett.* 75 (1995) 3728.
- [4] A. Al Salman, Spectroscopy and kinetic studies of electron–hole recombination in CdSe nanoparticles: effect of size, shape, and lattice structure, PhD Thesis, Ecole polytechnique Fédérale de Lausanne, 2007.
- [5] M. Shim, P. Guyot-Sionnest, *J. Chem. Phys.* 111 (1999) 6955.
- [6] Mark E. Schmidt, A. Sean Blanton, M.A. Hines, P. Guyot-Sionnest, *J. Chem. Phys.* 106 (1997) 5253.
- [7] F. van Mourik, G. Giraud, D. Tonti, M. Chergui, G. van der Zwan, *Phys. Rev. B* 77 (2008) 165303.
- [8] Liang-shi Li, A. Paul Alivisatos, *Phys. Rev. Lett.* 90 (2003) 097402.
- [9] T. Nann, J. Schneider, *Chem. Phys. Lett.* 384 (2004) 150.
- [10] D.V. Talapin, A.L. Rogach, A. Kornowski, M. Haase, H. Weller, *Nano Lett.* 1 (2001) 207.
- [11] Z.A. Peng, X.G. Peng, *J. Am. Chem. Soc.* 124 (2002) 3343.
- [12] A. Al Salman, A. Tortschanoff, M.B. Mohamed, D. Tonti, F. van Mourik, M. Chergui, *Appl. Phys. Lett.* 90 (2007) 09310.
- [13] S.A. Crooker, T. Barrick, J.A. Hollingsworth, V.I. Klimov, *Appl. Phys. Lett.* 82 (2003) 2793.
- [14] C. de Mello Donegá, M. Bode, A. Meijerink, *Phys. Rev. B* 74 (2006) 085320.
- [15] S.F. Wuister, A. van Houselt, C. de Mello Donegá, D. Vanmaekelbergh, A. Meijerink, *Angew. Chem. Int. Ed.* 43 (2004) 3029.
- [16] D. Tonti, F. van Mourik, M. Chergui, *Nano Lett.* 4 (2004) 2483.
- [17] M. Califano, A. Franceschetti, A. Zunger, *Nano Lett.* 12 (2005) 2360.
- [18] C. de Mello Donegá, C. Bode, M. Meijerink, *Phys. Rev. B* 74 (2006) 085320.
- [19] S. Shanbhag, N.A. Kotov, *J. Phys. Chem. B* 110 (2006) 12211.
- [20] C. Bonati, M.B. Mohamed, D. Tonti, G. Zgrablic, S. Haacke, F. van Mourik, M. Chergui, *Phys. Rev. B* 71 (2005) 205317.

- [21] S.-J. Park, S. Link, W.L. Miller, A. Gesquiere, P.F. Barbara, *Chem. Phys.* 341 (2007) 169.
- [22] B.R. Fischer, H.-J. Eisler, N.E. Stott, M.G. Bawendi, *J. Phys. Chem. B* 108 (2004) 143.
- [23] M. Kuno, D.P. Fromm, H.F. Hamann, A. Gallagher, D.J. Nesbitt, *J. Chem. Phys.* 112 (2000) 3117.
- [24] I. Chung, J.B. Witkoskie, J.G. Cao, M.G. Bawendi, *Phys. Rev. E* 73 (2006) 011106.
- [25] A.V. Malko, A.A. Mikhailovsky, M.A. Petruska, J.A. Hollingworth, V.I. Klimov, *J. Phys. Chem. B* 108 (2004) 5250.
- [26] K.-S. Cho, V. Dmitri, D.V. Talapin, W. Gaschler, C.B. Murray, *J. Am. Chem. Soc.* 127 (2005) 7140.
- [27] O. Schšps, N. Le Thomas, U. Woggon, M.V. Artemyev, *J. Phys. Chem. B* 110 (2006) 2074.
- [28] A. Al Salman, A. Tortschanoff, D. Tonti, F. Van Mourik, M. Chergui, submitted for publication.